A Broad-band End Launch Double Ridge Waveguide to Coaxial Transition Using LPDA

Maziar Hedayati, Mohsen Abdolahi, Hamid Mirmohammad Sadeghi, Parisa Moslemi, and Gholamreza Askari
Information and Communication Technology Institute (ICTI)
Isfahan University of Technology (IUT), Isfahan 84156, Iran

Abstract— In this paper, a wideband end launch ridge waveguide to coaxial transition is proposed, which operates in $8 \sim 14$ GHz. The microwave characteristics of double-ridge waveguide to coaxial transition are analyzed and simulated by full-wave analysis. Quarter wavelength Chebyshev impedance matching method used to design the middle part of the transition. Dimensions of the first part of transition have been calculated by time domain solver of Ansoft Designer based on finite element method (FEM). The compact LPDA is designed on microstrip to receive signal from the waveguide. This antenna is placed in the E-plane of the ridge waveguide to stimulate the TE_{10} dominant mode. Higher modes propagation can disturb the performance of the wide band transition. Also in this paper a C shape part is used to increase the cut off frequency of higher modes. The simulation results show that the S_{11} of the transition is below -10 dB in 8–14 GHz.

1. INTRODUCTION

Waveguide to Coaxial transition, as an important passive component has wide application in antennas radars and microwave systems Nowadays, broad band transitions are necessary for feeding wideband antenna in developing of the microwave systems. Most of designs like aperture-coupled slot [1] or aperture coupled patch element [2] have been expanded in the literature to introduce a useful transition from waveguide to microstrip. Although aperture-coupled structures are compact, but their fractional bandwidth is compact. Besides, the waveguide to microstrip transition based on the coupled probe at the E-plane [3] has been presented which is small but its bandwidth is limited ($\sim 22\%$ for less than -15 dB return loss). To modify the bandwidth, [4] has proposed transition using the stepped waveguides and [5] has presented the short-circuited tapered finline to widen the band width. However, the circuit size is also large. To decrease the size of the circuit, some researchers use the aperture slot coupling [6], and patch element [7] as a transition. The circuit size of these transitions can be reduced but in cost of narrow bandwidth. To enhance the bandwidth, waveguide to microstrip transitions using the open-circuited probe [8] and tapered coplanar strip (CPS) probe [9] were presented. But there is an additional slotline to microstrip transition in their designs. Furthermore, although [10] has presented a compact and broadband waveguide to microstrip transition using the anti-symmetric tapered probes, but there is an imbalance problem while transitioning from the ML to the rectangular waveguide. All of those transitions have been designed for simple rectangular waveguides, but for wideband application the ridge waveguides are more useful than rectangular waveguides which is not commonly presented any transition for them in the literatures.

2. TRANSITION DESIGN

The transition is designed for a double ridge waveguide with inner dimension $25.33\,\text{mm} \times 12.43\,\text{mm}$. The substrate with $\varepsilon r = 4.4$, $\tan\delta = 0.0009$, and thickness of 0.8 mm was used for planar circuit. The transition consists of three consecutive in-line sections including a double ridge waveguide, a Chebyshev matching and one LPDA. The substrate is placed in E-plane of waveguide and substrate plane must be parallel to waveguide propagation direction. An overall layout of the designed waveguide to coaxial transition is shown in Fig. 1.

2.1. Characterization of Ridge Waveguide

The dominant mode of ridge waveguide is TE_{10} mode, which is the same in rectangular waveguide. The cut of frequency TE_{10} mode of proposed ridge waveguide is 2 GHz. According to the transverse resonance condition, the cutoff wavelength (λ_c) of the ridge waveguide that works in the TE_{n0} mode can be calculated. The waveguide cross-section is shown in Fig. 2 and dominant mode and higher modes with different cut off frequency are shown in Fig. 3. As it can be seen, higher modes are propagated from 12 GHz that will effect on performance of transition. For suppressing higher modes

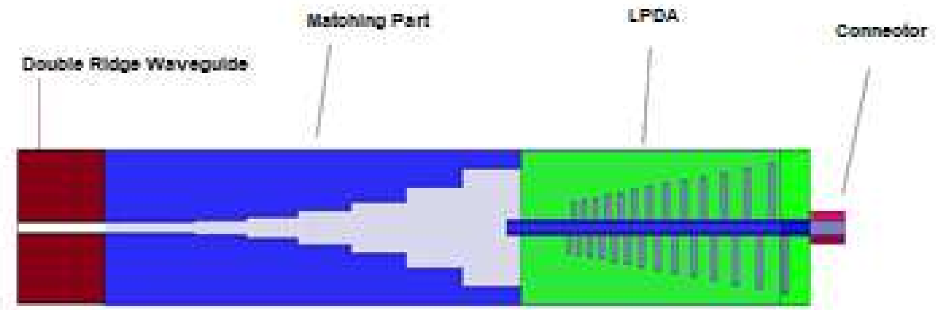

Figure 1: The layout of the proposed coaxial-to-waveguide transition.

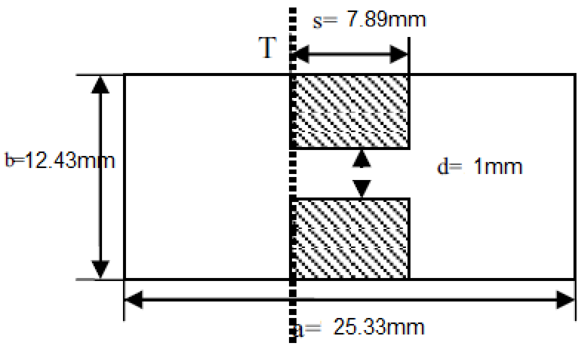

Figure 2: The size of ridge waveguide cross section.

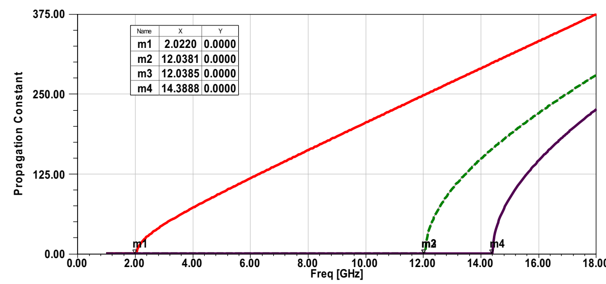

Figure 3: The Dominant mode and higher modes.

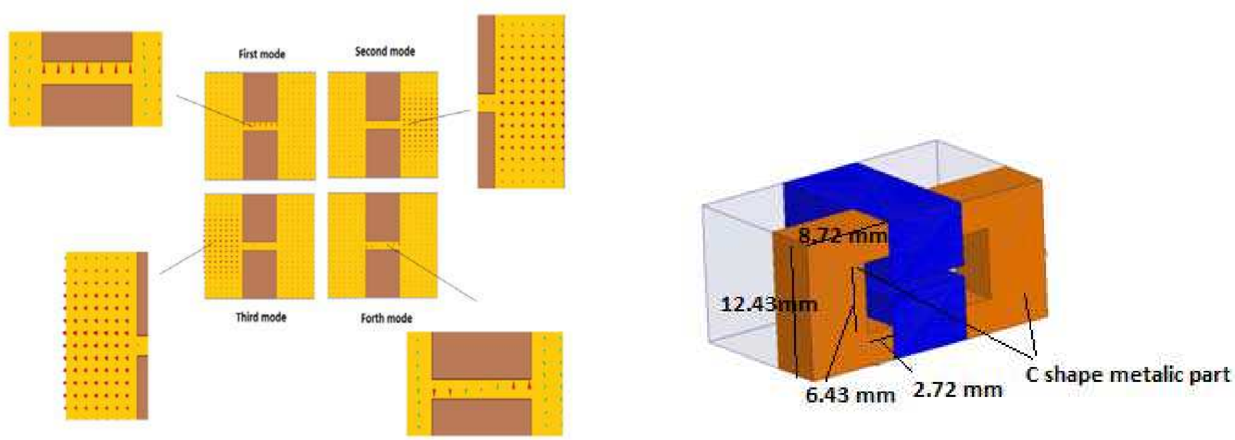

(a) (b)

Figure 4: (a) The field of four first mode. (b) The C-shaped metallic part.

in the frequency range a C-shaped metallic part (Fig. 4) added to waveguide and as it is depicted in Fig. 5 higher modes will start on upper frequency near 17 GHz that is out of frequency performance.

The impedance of ridge waveguide depended on frequency because it is a non-TEM transmission line. So, the characteristic impedance can be expressed by the impedance at infinite frequency and the wavelengths of the waveguide [11]:

$$Z(w) = Z(\infty) \cdot \frac{\lambda_g}{\lambda_c} = \frac{Z(\infty)}{\sqrt{1 - \left(\frac{\lambda_0}{\lambda_c}\right)}} \qquad (1)$$

where $Z(\infty)$ is the waveguide characteristic impedance of infinity frequency; λ_0 is the wavelength of free-space and λ_c is the cut-off wavelength of waveguide.

The power-voltage characteristic impedance is defined as:

$$Z_{OPV} = \frac{V_0^2}{2P} \tag{2}$$

where V_0 the peak voltage between two ridges and P is the average power propagated in z direction. The characteristic impedance of any frequency can be got through (3):

$$Z_{OPV}(w) = \frac{Z_{PV}^{\infty}}{\sqrt{1 - \lambda/\lambda_c}} \tag{3}$$

where Z_{PV}^{∞} the impedance of infinite frequency and its expression is:

$$Z_{OPV}^{\infty}(w) = \frac{1}{\frac{k}{120\pi^2\beta}\left\{\begin{array}{l} m\frac{2\beta}{k}\cos^2\frac{\pi\gamma}{k}\ln\csc\frac{\pi d}{2b} + \frac{\pi\gamma}{2k} + \frac{1}{4}\sin\frac{\pi\gamma}{k} \\ +\frac{d}{b}\frac{\cos^2\frac{\pi\gamma}{k}}{\sin^2\frac{2\pi\delta}{k}}\left[\frac{\pi\delta}{k} - \frac{1}{4}\sin\frac{4\pi\delta}{k}\right] \end{array}\right\}}$$

$$k = \frac{\lambda_c}{a};\ \beta = \frac{d}{a};\ \gamma = \frac{s}{a};\ \delta = \frac{(1 - s/a)}{2} \tag{4}$$

We can get the theoretical characteristic impedance of any frequency required by formula (1)∼(4). Now it is possible to calculate the value of the impedance at each frequency from the formula (Fig. 6).

2.2. Design of the Matching Structure

There are several matching methods, but with consideration of the manufacturing cost in this paper a quarter wavelength Chebyshev matching method is adopted. With the formula in Section 2.1, the input and output impedance are obtained: $Z = 37.6\,\Omega$, $Zn_{+1} = 275\,\Omega$. From the design table, six section transition is enough to achieve this purpose. The impedance of each section is: $Z_1 = 43.3\,\Omega$, $Z_2 = 57\,\Omega$, $Z_2 = 88.6\,\Omega$, $Z_2 = 122\,\Omega$, $Z_2 = 169\,\Omega$, $Z_2 = 234.5\,\Omega$. Each branch ridge has the same width (7.89 mm). Table 1 shows the dimensions of each section's gap and length. This matching structure is depicted in Fig. 7. The simulation results of this part is shown in Fig. 8. As it is shown in figure, return loss is more than 12 dB and insertion loss is smaller than 0.2 dB that shows good matching.

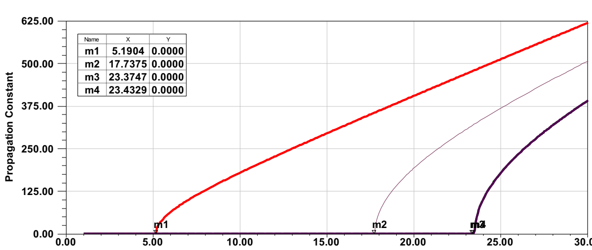

Figure 5: The dominant mode and higher modes with C-shaped metallic part.

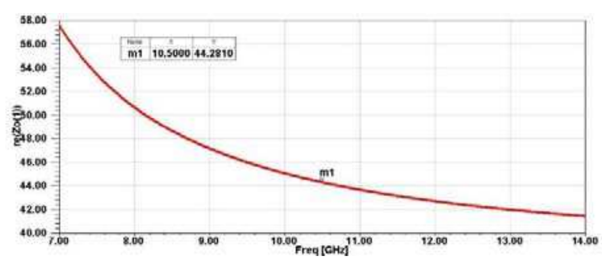

Figure 6: The characteristic impedance at each frequency.

Table 1: The dimensions and the characteristic impedance of transition.

	Gap	Length	Characteristics Impedance
	d (mm)	L (mm)	Z_0 (Ω)
First branch	1.23	7.3	43.3
Second Branch	1.63	7.3	57
Third branch	2.83	7.49	88.6
Fourth branch	4.23	7.65	122
Fifth	6.43	7.92	169
Sixth	9.41	8.27	234.5

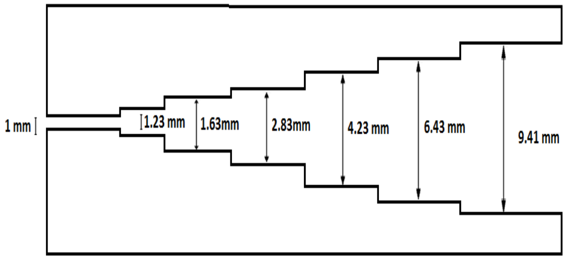

Figure 7: The matching structure and its dimensions.

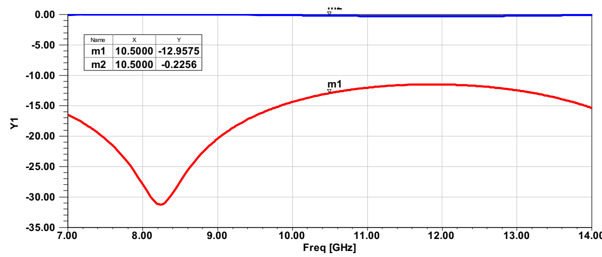

Figure 8: The simulation result of matching structure.

2.3. LPDA Design

Figure 9 shows the configuration of the proposed antenna. The antenna was designed on both sides of the 0.8 mm thick substrate with a dielectric constant 4.4 and loss tangent 0.0009. The antenna is designed to cover the X band and upper from 8 GHz to 14 GHz. With the desired directivity set at 10 dBi, the scaling factor and spacing factor were determined to be 0.96 and 0.1 based on the corrected Carrel's tables. As it is known, the dielectric can lead to reduction in size and gain of antenna. Since, the effective dielectric constants are not the same in every region of a PLPDA antenna, two effective dielectric constants should be considered to scale the dimensions. For a substrate with $\varepsilon r = 4.4$, they are chosen about 3.5 and 1.5, respectively. The return loss of antenna has been illustrated in Fig. 10 and obvious return loss is less than 10 dB in 8–14 GHz frequencies.

3. SIMULATION RESULTS

The double ridge waveguide to coaxial transition is designed by using two individually optimized components together (LPDA and matching network) to achieve optimum performance. One prototype have been designed and simulated using dielectric with $\varepsilon_r = 4.4$ and substrate thickness of 0.8 mm. The printed antenna pattern is located at the center of the waveguide. The transition was modeled and analyzed with Ansoft HFSS 12.0 which is shown in Fig. 11. The return loss is better

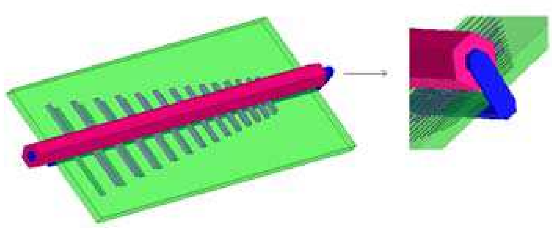

Figure 9: The designed LPDA.

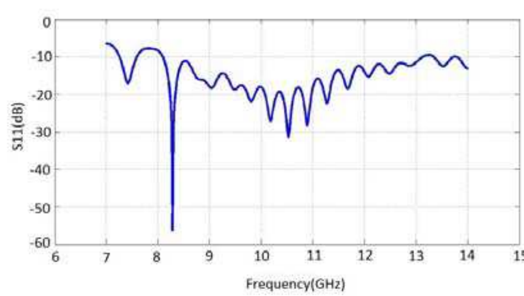

Figure 10: The return loss of antenna.

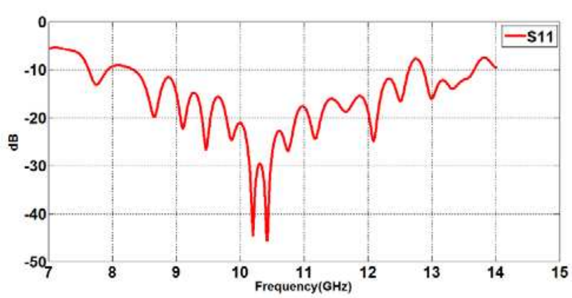

Figure 11: The return loss of final transition.

than 12 dB in X-band and better than 10 dB in the whole 8–14 GHz.

4. CONCLUSION

A broad band end launcher ridge waveguide to coaxial transition using a LPDA has been proposed and demonstrated in this paper. The transition's mechanism is presented in detail for every components to understand its broad-band characteristics. The 10 dB fractional bandwidth of the waveguide-to-coaxial transition covers the frequency range 8–14 GHz, which is calculated to be 51%.

REFERENCES

1. Das, B. N., K. V. S. V. R. Prasad, and K. V. Seshagiri Rao, "Excitation of waveguide by stripline- and microstrip-line-fed slots," *IEEE Trans. Microw. Theory Tech.*, Vol. 34, No. 3, 321–327, Mar. 1986.
2. Grabherr, W. and W. Menzel, "A new transition from microstrip line to rectangular waveguide," *Proc. 22th Eur. Microw. Conf.*, 1170–1175, Sep. 1992.
3. Lou, Y., C. H. Chan, and Q. Xue, "An in-line waveguide-to-microstrip transition using radial-shaped probe," *IEEE Microw. Wireless Compon. Lett.*, Vol. 18, No. 5, 311–313, May 2008.
4. Yao, H.-W., A. Abdelmonem, J.-F. Liang, and K. A. Zaki, "Analysis and design of microstrip-to-waveguide transitions," *IEEE Trans. Microw. Theory Tech.*, Vol. 42, No. 12, 2371–2380, Dec. 1994.
5. Van Heuven, J. H. C., "A new integrated waveguide-microstrip transition," *IEEE Trans. Microw. Theory Tech.*, Vol. 24, 144–147, 1976.
6. Herrero, P. and J. Schoebel, "A WR-6 rectangular waveguide tomicrostrip transition and patch antenna at 140 GHz using low-cost solutions," *Proc. IEEE Radio and Wireless Symp.*, 355–358, Orlando, FL, USA, 2008.
7. Wu, P., Z. Wang, Y. Zhang, S. Sun, and R. Xu, "Wideband waveguide-to-microstrip probe transition with LTCC technology," *Electron. Lett.*, Vol. 47, No. 1, 43–44, 2011.
8. Lou, Y., C. H. Chan, and Q. Xue, "An in-line waveguide-to-microstriptransition using radial-shaped probe," *IEEE Microw. Wirel. Compon. Lett.*, Vol. 18, No. 5, 311–313, 2008.
9. Lin, T.-H. and R.-B. Wu, "A broadband microstrip-to-waveguidetransition with tapered CPS probe," *Proc. 32nd Eur. Microwave Conf.*, 1–4, Milan, Italy, 2002.
10. Chuang, J.-K., R.-Y. Fang, and C.-L. Wang, "Compact and broadband microstrip-to-waveguide transition using antisymmetric tapered probes," *Electron. Lett.*, Vol. 48, No. 6, 332–333, Mar. 2012.
11. Nie, R.-X., E. Li, G.-F. Guo, and Y. Wang, "Simulation and design of 18–40 GHz ridge waveguide to coaxial transition," *2011 IEEE International Conference on Microwave Technology & Computational Electromagnetics (ICMTCE)*, 183–185, May 22–25, 2011.